

hep-th/0304241
 HIP-2003-28/TH
 CERN-TH/2003-097
 November 20, 2003

The Taming of Closed Time-like Curves

Rahul Biswas^{3*}, Esko Keski-Vakkuri^{1†}, Robert G. Leigh^{2,3‡},
 Sean Nowling^{3§} and Eric Sharpe^{3¶}

¹*Helsinki Institute of Physics
 P.O. Box 9, FIN-00014 University of Helsinki, Finland*

²*CERN-Theory Division
 CH-1211, Geneva 23, Switzerland*

³*Department of Physics, University of Illinois
 1110 W. Green Street, Urbana, IL 61801, U.S.A.*

Abstract

We consider a $\mathbb{R}^{1,d}/\mathbb{Z}_2$ orbifold, where \mathbb{Z}_2 acts by time and space reversal, also known as the embedding space of the elliptic de Sitter space. The background has two potentially dangerous problems: time-nonorientability and the existence of closed time-like curves. We first show that closed causal curves disappear after a proper definition of the time function. We then consider the one-loop vacuum expectation value of the stress tensor. A naive QFT analysis yields a divergent result. We then analyze the stress tensor in bosonic string theory, and find the same result as if the target space would be just the Minkowski space $\mathbb{R}^{1,d}$, suggesting a zero result for the superstring. This leads us to propose a proper reformulation of QFT, and recalculate the stress tensor. We find almost the same result as in Minkowski space, except for a potential divergence at the initial time slice of the orbifold, analogous to a spacelike Big Bang singularity. Finally, we argue that it is possible to define local S-matrices, even if the spacetime is globally time-nonorientable.

*E-mail: rbiswas@students.uiuc.edu

†E-mail: esko.keski-vakkuri@helsinki.fi

‡E-mail: rgleigh@uiuc.edu

§E-mail: nowling@students.uiuc.edu

¶E-mail: ersharpe@uiuc.edu

1 Introduction and Summary

A technical obstacle in exploring string theory in time-dependent space-times is to find suitable backgrounds where string quantization is tractable. Early work includes [1] – [6]. More recently, interest has been revitalized, motivated in part by novel string-based cosmological scenarios (see for example [7, 8, 9]). An obvious path to follow was to construct such backgrounds as time-dependent orbifolds of Minkowski space [10] – [18] or anti-de Sitter space [19, 20, 21]. Further related work includes [22] – [32]. However, depending on how the orbifold identifications are defined, potentially dangerous issues may arise. The resulting time-dependent orbifolds can have regions with closed time-like curves (CTCs) or closed null curves (CNCs), or may not even be globally time-orientable. Therefore, one could choose to first make a list of desirable features for the orbifolds and then try to limit the study only to those backgrounds that possess those features. This sensible strategy was laid out and pursued by Liu, Moore and Seiberg [14, 15]. For orbifolds of type $\mathbb{R}^{1,3}/\Gamma$ where Γ is a discrete subgroup of the Poincaré group, the list turned out to be very short containing only the null branes with $R > 0$. However, the null brane construction involves identifications by arbitrarily large boosts. This turns out to be another potential reason for instabilities, and it was argued by Horowitz and Polchinski [16] that such backgrounds become unstable after just a single particle is added, because on the covering space the particle can approach its infinitely many images with increasingly high momenta and produce a black hole. Additional discussion of potential problems can be found in [17, 15, 26].

Aside from constructing and studying time-dependent backgrounds by alternative methods, one might speculate if the list of desirable features for suitable orbifold backgrounds was too prohibitive and reconsider the reasons for including each item on the list. In any case, it is important to understand if and/or why string theory actually has problems with these features. The reason for demanding that there be no regions containing closed time-like curves appears obvious. Classically, CTCs violate causality, and quantum mechanically, coherence and unitarity come into question. It has been conjectured by Hawking [33] that the laws of physics prevent CTCs from appearing if they do not exist in the past. The arguments in support of this chronology protection conjecture (CPC) are usually based on general relativity plus matter at the classical or semiclassical level. A recent summary can be found in [34]. Essential features are that perturbations can keep propagating around a CTC so that backreaction accumulates, or quantum effects can lead the matter stress tensor to diverge at the boundary of the CTC region, leading to infinite backreaction. However, the trouble with CTCs and CNCs seems to arise from propagation along them, rather than merely from their existence. It is not clear if the two are equivalent. For example, the model studied in [10] involves CTCs and CNCs,

but it was argued that they do not necessarily pose a problem in quantum mechanics if one can project to a subspace of states which do not time evolve along the CTCs and CNCs. Another desirable feature on the list was time-orientability. This was included to avoid problems in defining an S-matrix, and problems associated with the existence of spinors [35, 36, 37]. However, the consequences of a lack of time-orientability have not yet been subject to extensive investigation and are thus less well understood. From the point of view of local physics, one might wonder if the whole Universe could be globally time-nonorientable, but in such a way that the global feature could only be detected by meta-observers and never be revealed by local experiments. The orbifold studied in [10] is an example of a spacetime which is globally time-nonorientable. In any case, its structure appears to allow for a definition of an S-matrix for local experiments.

To summarize, there are many reasons to investigate the chronology protection conjecture and time-nonorientability. We also note that recently the former topic has been investigated from other points of view in the context of string theory and holography [38, 39, 40, 41, 42]. The $\mathbb{R}^{1,d}/\mathbb{Z}_2$ orbifold, obtained by identifying points X with reflected points $-X$, provides a simple model which incorporates both issues. Some comments were made in passing in [10]. In this paper we perform a more detailed investigation.

The orbifold is also relevant for the elliptic interpretation of de Sitter space (dS) [43, 44, 45, 46]. A d -dimensional de Sitter space is a time-like hyperboloid embedded in $\mathbb{R}^{1,d}$. The \mathbb{Z}_2 reflection on $\mathbb{R}^{1,d}$ induces an antipodal reflection on the dS spacetime. The elliptic de Sitter space dS/\mathbb{Z}_2 is then defined by identifying the reflected antipodal points.

The identification leads to various problems in quantum field theory. Previous studies of the elliptic dS spacetime have discussed problems in defining a global Fock space in the global patch; however, it was possible to construct QFT and a Fock space by restricting to the static patches of observers at the (identified) north and south poles. The same problem is encountered in trying to formulate QFT on $\mathbb{R}^{1,d}/\mathbb{Z}_2$. Moreover, there is a question of whether the orbifold is an unstable background. One can present a quick semiclassical derivation of the stress energy and find that it diverges; for example in the case of a massless scalar field one obtains a divergence in the lightcone emanating from the origin.

We show that these problems can be circumvented after one formulates quantum field theory in a manner which appropriately incorporates the \mathbb{Z}_2 identification under time reversal and space reflection. We argue that in such a formulation one needs to first double the field degrees of freedom, with the copy fields propagating towards the reversed time direction, and then identify the degrees of freedom under the \mathbb{Z}_2 reflection. The doubling of fields is motivated by (the zero temperature limit of) the real-time formulation of finite temperature QFT. The doubling of degrees of freedom helps to overcome problems with causality when the light-cones of the identified points X and $-X$ intersect, as we will

assume that the two copies of the fields (at X and $-X$) are dynamically decoupled. Note that in the limit in which the cosmological constant approaches zero, the dS spacetime becomes locally Minkowski spacetime. Correspondingly, it has been argued that in this limit the elliptic dS spacetime goes to two copies of Minkowski spacetime, related by the \mathbb{Z}_2 reflection [46]. In the present work, we would instead propose that QFT on the elliptic dS spacetime goes to QFT on $\mathbb{R}^{1,d}/\mathbb{Z}_2$, with two copies of *fields*, identified under the \mathbb{Z}_2 reflection.

We also study the backreaction at one-loop level in string theory. We calculate the one-loop graviton tadpole in the $\mathbb{R}^{1,d}/\mathbb{Z}_2$ background, and show that the answer is the same as if the background were just $\mathbb{R}^{1,d}$! While the answer first appears puzzling, it appears very natural in relation to the \mathbb{Z}_2 invariant formulation of QFT. Indeed, the low-energy limit of string theory should be the \mathbb{Z}_2 invariant QFT.

Finally, we argue that it is possible to define S-matrices in a manner that makes sense locally. The definition only breaks down at the point which can be regarded as the initial “Big Bang singularity” of the orbifold, and at that point we also find that even in the invariant reformulation of the QFT, the stress tensor diverges. However, it is also possible that stringy effects lead to a smooth blow-up of the orbifold singularity. Then the QFT would need to be reconsidered in this smooth background.

We have organized the paper as follows. In Section 2, we review some features of the time-dependent orbifold background, and focus on some novel features of these orbifolds. In particular, we point out that a choice of time orientation must be made. In Section 3, we review the (naïve) analysis of the gravitational back reaction in this geometry. In Section 4, we ask if string theory can do better, and present similar calculations in string theory (complementary calculations in a different formalism are shown in the Appendix.). We find that the result differs significantly from the naïve QFT analysis. To resolve the puzzle, in Section 5, we present a proper formulation of quantum field theory on the $\mathbb{R}^{1,d}/\mathbb{Z}_2$ background. We show that the result now contains the familiar short-distance Minkowski spacetime divergence, in agreement with the string calculation, plus an additional divergence, which can be interpreted as a “cosmological initial condition.” The latter does not arise from the first quantized string calculation and would need a more involved analysis to understand as a low energy limit of string theory. Finally, in Section 6, we discuss further features of the interacting QFT, including a discussion of the S-matrix.

2 Overview of $\mathbb{R}^{1,d}/\mathbb{Z}_2$

Let us first review some features of the $\mathbb{R}^{1,d}/\mathbb{Z}_2$ orbifold [10]. We begin with the covering space $\mathbb{R}^{1,d}$ and identify the time and space coordinates under the reflection

$$(t, x^a) \sim (-t, -x^a) . \quad (1)$$

The resulting orbifold is a space-time cone, depicted in Figure 1 for $d = 1$. Points in the opposite quadrants (I and III, and II and IV) are identified. Orbifolds that act purely

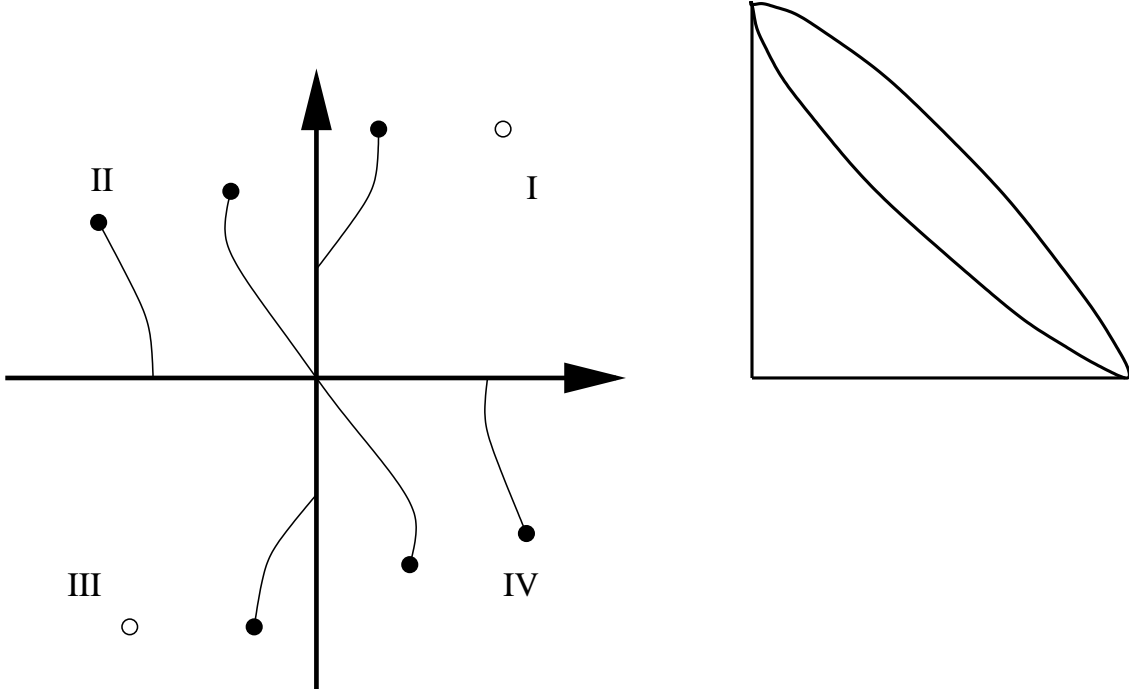


Figure 1: The orbifold $\mathbb{R}^{1,1}/\mathbb{Z}_2$. Also depicted are some identified points and resulting closed timelike curves.

spatially are familiar and are certainly well understood. New problems arise when the identification involves the time direction; for example it is not guaranteed that the string spectrum will be free from tachyons and ghosts. Ref. [10] investigated bosonic and type II superstrings on $\mathbb{R}^{1,d}/\mathbb{Z}_2 \times \mathbb{R}^n$, with n additional spacelike directions added to bring the total spacetime dimension to 26 or 10. It was shown, using a Euclidean continuation, that although the background is time-dependent and quantization had to be done in the covariant gauge, the physical spectrum did not contain any negative norm states (ghosts), at least in a range of d . The superstring spectrum did not contain any tachyons and the one-loop partition function vanishes for the superstring.

Although string theory passed the first tests, questions associated with the time identification on the orbifold remained. In the orbifold (1), there is actually extra data that must be specified. To see this, we note that to specify a Lorentzian metric on an orientable space M ($w_1(M) = 0$), we must specify a *time orientation*. Mathematically, this implies a real rank 1 subbundle $L \subset TM$, the time orientation bundle. (M is said to be globally time-orientable when $w_1(L) = 0$.) A time-like Killing vector defining time's arrow, if available, would be a global section of this line bundle.

In the case of the orbifold (1), we must ask how various quantities descend from the covering space to the orbifold. In particular, $\partial/\partial t$ is manifestly not invariant under the group action, and so does not define a time's arrow, or time-like Killing vector, in the quotient. Thus, this orbifold leaves ambiguous the direction on which time flows in the quotient – we must manually make a choice of direction of time-flow.

Furthermore, the natural time orientation bundle on the covering space does descend to the quotient space, but (omitting the singularity at the origin) the class $w_1(L)$ is non-trivial. Thus the image of L on the quotient is not time-orientable. Although locally we can choose a perfectly sensible notion of time orientation, this is not possible globally.

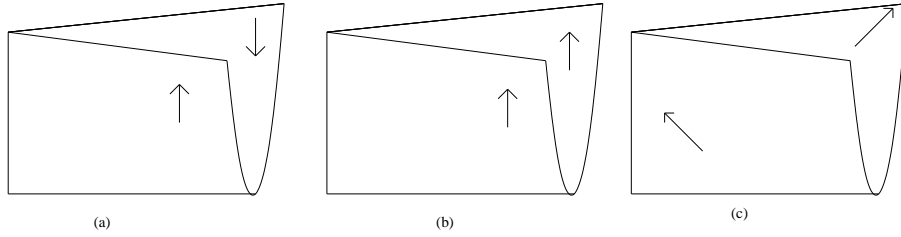


Figure 2: Three possible time-arrows on the quotient $\mathbb{R}^{1,1}/\mathbb{Z}_2$.

To illustrate, let us consider the case of $\mathbb{R}^{(1,1)}/\mathbb{Z}_2$. The obvious choice of time's arrow on the covering space $\mathbb{R}^{1,1}$, namely $\partial/\partial t$, is not invariant under the group action, a property which manifests itself in the observation that by picking different fundamental domains for the group action on the cover, the time's arrow in those fundamental domains restricts to a different time's arrow on the quotient.

In Fig. 2 we have shown three possible time-arrows that one can construct on $\mathbb{R}^{1,1}/\mathbb{Z}_2$. The left-most case corresponds to taking the fundamental domain to be regions I and IV, the middle case corresponds to taking the fundamental domain to be regions I and II, and the right-most case corresponds to taking the fundamental domain to be one side of a wall of the lightcone through the origin. In each case, omitting the origin, the time-orientation line bundle on the quotient is not orientable ($w_1(L) \neq 0$), hence each choice of time's arrow depicted in figure 2 has zeroes – in case (a), along the left vertical crease,

and in case (b), along the bottom horizontal crease. Note that in each case it would also be possible to choose a reverse time orientation (reversed arrows). Then *e.g.* Fig. 2(b) would depict a “big crunch” rather than a “big bang.”

In Figure 3, we have drawn the quotient space corresponding to Fig. 2(a). In this case, there are asymptotic regions for both $t \rightarrow \pm\infty$. However, there is a topology change of constant t slices at $t = 0$. Another choice for the quotient space, corresponding to Fig.

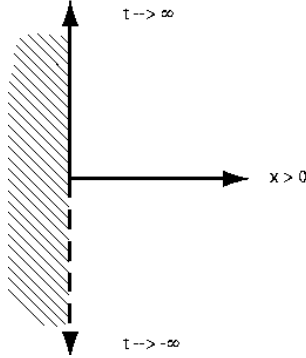


Figure 3: A view of the quotient spacetime (for 1+1 dimensions). Note the absence of the $x = 0$ axis for $t < 0$.

2(b), is shown in Fig. 4. In this case, there is no asymptotic region corresponding to $t \rightarrow -\infty$. Instead, we have a “big bang” singularity at $t = 0$. It is interesting to

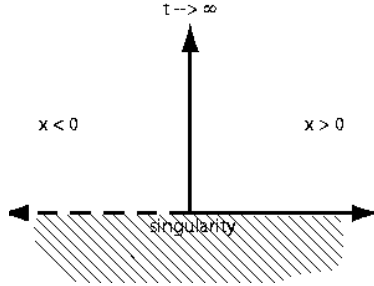


Figure 4: Another view of the quotient spacetime (for 1+1 dimensions). Note the absence of the $t = 0$ axis for $x < 0$. The $t = 0$ axis represents a “big bang” singularity—the beginning of the spacetime.

contemplate the properties of quantum field theory on such a spacetime. It is of even more interest to ponder the role of string theory. We will return to a more thorough discussion of these issues in a later section.

Let us also discuss the closed time-like curves in this geometry. In the covering space, with the natural choice of Minkowski time orientation, there are non-trivial forward oriented closed time-like curves. Examples are shown in Fig. 1. It is clear from the figure that there are CTC's which begin at any spacetime point.

Consider however these curves in the quotient space (let us refer to the choice of time-orientation in Fig. 2(a) to be definite). In going to the quotient we make a choice of (local) time orientation which is not compatible with the time orientation of the covering space. As a result (and this is true for any choice), the CTC's that we identified in the covering space are *not forward oriented* in the quotient. The examples given in Fig. 1 are redrawn in the quotient in Fig. 5. In fact, the only CTC in the quotient must begin and

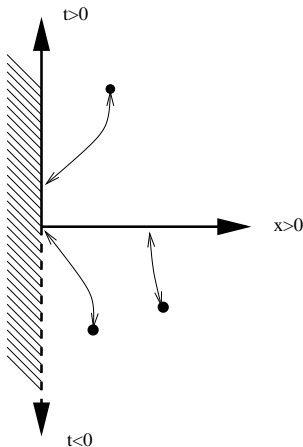


Figure 5: The CTC's of Fig. 1 are not forward oriented in the quotient.

end on the singular axis (the curve can be constructed by a limiting procedure.)

Let us quickly review this discussion. In the Lorentzian orbifold, a choice of time orientation must be made in the quotient.⁶ This gives rise to physically inequivalent spacetimes that are singular along an axis. The singularity is associated with an undefined time orientation. Whereas there were oriented CTC's through every point in the covering space, (almost) all of these are not forward oriented in the quotient. Next, we will consider quantum field theory on this background; we focus on the issue of back-reaction.

3 Backreaction in Quantum Field Theory

Here we give a short review of the standard QFT calculation for the vacuum expectation value (vev) of the stress tensor, which in general leads to a divergence hinting at an

⁶It is not clear how this choice should be encoded in string theory.

instability of the background. Later, we will contrast this with a calculation in string theory.

The gravitational backreaction from the renormalized stress energy of a quantum field may be evaluated semi-classically

$$G_{\mu\nu} = -8\pi G_N \langle T_{\mu\nu} \rangle_{ren}. \quad (2)$$

Here the subscript refers to the fact that one subtracts off the usual vacuum energy contribution — the curvature is well-defined if there are no divergences other than the usual flat space short distance singularities. In more detail [34], one defines the renormalized stress tensor starting from the two-point correlation function $G(x, y)$ written in Hadamard form as a sum over geodesics γ from x to y . The expectation value of the point-split stress tensor can then be defined as

$$\langle T_{\mu\nu}(x, y, \gamma_0) \rangle = D_{\mu\nu}(x, y, \gamma_0) G(x, y), \quad (3)$$

where γ_0 denotes the trivial geodesic from x to y which collapses to a point as $y \rightarrow x$, and $D_{\mu\nu}(x, y, \gamma_0)$ is the second order differential operator associated with the action of the particular field in scrutiny. The renormalized stress energy $\langle T_{\mu\nu}(x) \rangle_{ren}$ is defined by discarding the universal divergent piece arising from the contribution of the trivial geodesic to the Green function. That is, one replaces in (3) the Green function by the renormalized Green function, defined with the trivial geodesic excluded from the sum over geodesics:

$$G(x, y) = \sum_{\gamma} \cdots \rightarrow G_{ren}(x, y) = \sum_{\gamma \neq \gamma_0} \cdots, \quad (4)$$

and then removing the point-splitting regularization from (3) by taking the limit $\lim_{y \rightarrow x}$.

Let us then consider the $\mathbb{R}^{1,1}/\mathbb{Z}_2$ orbifold and *e.g.* the stress energy of a free massless scalar field. The field decomposes into left- and right-movers. Let us focus on the right-movers only. The right-moving component of the stress tensor is

$$T_{uu}(u) =: \partial_u \phi(u) \partial_u \phi(u) :, \quad (5)$$

where $u = t - x$. To proceed as in the above, we start from the Minkowski space two-point correlation function

$$G(u, u') \sim -\ln(u - u'), \quad (6)$$

associated with the trivial geodesic from (u, v) to (u', v') . On the orbifold, the points (u, v) are identified with $(-u, -v)$ and (u', v') identified with $(-u', -v')$. This gives rise to three additional geodesics (Fig. 6), so the two point function on the orbifold would be

$$G_{orb}(u, u') = G(u, u') + G(u, -u') + G(-u, u') + G(-u, -u'). \quad (7)$$

Subtracting off the trivial universal divergence, we then obtain the renormalized stress energy

$$\begin{aligned}\langle \tilde{T}_{uu}(u) \rangle_{ren} &= \lim_{u' \rightarrow u} \partial_u \partial_{u'} \{ -\ln(u - u') - \ln(u + u') \}_{ren} \\ &= \lim_{u' \rightarrow u} \frac{1}{(u + u')^2} = \frac{1}{4u^2} .\end{aligned}\tag{8}$$

However, the result is divergent on the null line $u = 0$. The problem arises from the non-trivial geodesics which can also become zero length (see Fig. 6). A similar calculation for the left-movers yields a divergence at $v = 0$. Hence one concludes that the orbifold is potentially unstable. Similar calculations can be done in higher dimensions.

However, upon closer inspection the above argument has some puzzling features. If we want to associate the two-point function (7) with a field operator, the operator should be symmetric under the $u \rightarrow -u$ \mathbb{Z}_2 reflection. A naive way to impose the invariance is to consider

$$\tilde{\phi}(u) = \frac{1}{\sqrt{2}}(\phi(u) + \phi(-u)) .\tag{9}$$

Formally, one can check that the renormalized expectation value (8) is that of the \mathbb{Z}_2 invariant field operator, with the four contributions associated with 'short' and 'long' contractions. However, this construction has various problems. The most cumbersome

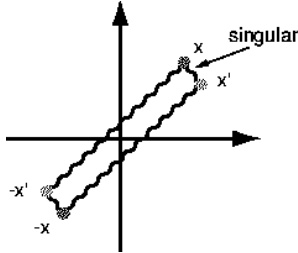


Figure 6: Correlator of point-split composite operator. The 'short' contractions, between x and x' are the usual short-distance ones, and should be subtracted. The 'long' contractions give rise to the Casimir energy.

one is that the \mathbb{Z}_2 invariant field operator (9) has the mode expansion

$$\tilde{\phi}(u) = \sqrt{2} \int d\omega (a_\omega + a_\omega^\dagger) \cos(\omega u)\tag{10}$$

so it is not clear what exactly is meant by the naive notion of particles and vacuum. The problem of constructing a global Fock space is also well known from investigations of elliptic de Sitter space dS/\mathbb{Z}_2 [43, 44, 45, 46]. In the above, the problem has been lifted onto $\mathbb{R}^{1,d}/\mathbb{Z}_2$, where the dS/\mathbb{Z}_2 can be embedded.

Actually, we will argue that the orbifold identification requires identifying a particle with positive energy at (t, x) with a particle with negative energy at $(-t, -x)$. Particles of the latter kind cannot be created with a_ω^\dagger . A quick look at the mode expansion of $\phi(-u)$ might give a false impression that this would happen, but really $\phi(-u)$ is just the field operator ϕ evaluated at point $-u$ rather than a new operator with the creation and annihilation operators acting in a different way. Another problem is that the usual prescription calls us to evaluate commutators of field operators at equal time. On the orbifold covering space this becomes problematic, since “equal time” now corresponds to times t and $-t$. For these reasons we would like to take a step back and reconsider the formulation of field theory on the $\mathbb{R}^{1,d}/\mathbb{Z}_2$ orbifold. However, we will first examine if the divergence of the stress tensor persists in string theory. The result that we find will provide additional motivation to reconsider the formulation of field theory.

4 The String Theory Calculation

Our next goal is to calculate the backreaction on the orbifold at one-loop level in string theory. In practice, this is done by calculating the one-loop graviton tadpole.

If we write the metric tensor as $g_{\mu\nu}(x) = \eta_{\mu\nu} + 2\kappa h_{\mu\nu}(x)$, the vev of the stress tensor may be written [47]

$$\langle T_{\mu\nu} \rangle = -i \frac{\delta}{\delta g^{\mu\nu}} \ln Z_{EFT}^{2nd} |_{h^{\mu\nu}=0} = -\frac{i}{2\kappa} \frac{\delta Z_{1st}}{\delta h^{\mu\nu}} |_{h^{\mu\nu}=0} . \quad (11)$$

In the above, we used the relation between the vacuum amplitudes in the second quantized and first quantized formalism, $Z_{2nd} = e^{Z_{1st}}$, to replace the effective field theory action $\ln Z_{EFT}^{2nd}$ by the point particle partition function Z_{1st} .

Now we replace point particles by strings. At one-loop level [48]

$$Z_{1-loop}^{ST}[g] = \int \frac{d\tau d\bar{\tau}}{4\tau_2} Z(\tau) = \int \frac{d\tau d\bar{\tau}}{4\tau_2} \int_{T^2} \mathcal{D}X e^{i\frac{T}{2} \int d^2w g_{\mu\nu}(X) \partial X^\mu \bar{\partial} X^\nu} . \quad (12)$$

This is then inserted in (11).⁷ Suppressing the integral over τ , we have

$$Z_{1-loop}^{ST} = \int \mathcal{D}X e^{i\frac{T}{2} \int d^2w \eta_{\mu\nu} \partial X^\mu \bar{\partial} X^\nu} \left\{ 1 + i \frac{g_{str}}{\alpha'} \int d^2w h_{\mu\nu}(X) \partial X^\mu \bar{\partial} X^\nu + \dots \right\} . \quad (13)$$

Now Fourier expand the perturbation,

$$h_{\mu\nu}(X) = \int \frac{d^{D+1}k}{(2\pi)^{D+1}} e_{\mu\nu}(k) e^{ik \cdot X} \quad (14)$$

⁷This is somewhat reminiscent of a recent calculation in [49].

and introduce

$$V_{\mu\nu}(k) = \partial X^\mu \bar{\partial} X^\nu e^{ik \cdot X} , \quad (15)$$

then

$$Z_{1-loop}^{ST}[g] = Z_{1-loop}^{ST}[\eta] + i \frac{g_{str}}{\alpha'} \int \frac{d^{26}k}{(2\pi)^{D+1}} \int d^2w e_{\mu\nu}(k) \langle V^{\mu\nu}(k; w) \rangle + \dots . \quad (16)$$

We then get

$$\langle T^{\mu\nu}(x) \rangle = \frac{1}{4\pi\alpha'} \int \frac{d^{D+1}k}{(2\pi)^{D+1}} \int d^2w \langle V^{\mu\nu}(k; w) \rangle e^{-ik \cdot x} \quad (17)$$

the relation between the Fourier transformed tadpole and the stress tensor.

Note that in Minkowski space, one obtains

$$\langle V^{\mu\nu}(k) \rangle = - \left(\frac{g_{str}}{4\pi\tau_2} \right) \frac{\delta^{(D+1)}(\sqrt{\alpha'}k)}{V_{D+1}} \eta^{\mu\nu} Z_{1-loop} , \quad (18)$$

so that

$$\langle T_{\mu\nu} \rangle \sim \frac{1}{\alpha'^{13} V_{26}} Z_{1-loop} \times \eta_{\mu\nu} \quad (19)$$

which is of the right form for the stress tensor of a cosmological constant $\Lambda \sim Z_{1-loop}$.

On \mathbb{Z}_2 orbifolds, the story is essentially similar. What is different in the string graviton tadpole calculation is that a) the relevant vertex operator must be \mathbb{Z}_2 invariant: it is the sum of vertex operators carrying k and $-k$ in the directions of the orbifold, and b) a priori there are contributions from the twisted sector strings. The fact a) suggests that the Fourier transform of the tadpole will be the sum

$$\langle T_{\mu\nu}(X) \rangle + \langle T_{\mu\nu}(-X) \rangle, \quad (20)$$

where X are the coordinates along the orbifold directions. This could be obtained from the effective action by including the functional differentiation $\delta/\delta h_{\mu\nu}(-X)$. We will return to these issues when we discuss the reformulation of QFT. Let us first proceed with the calculation of the tadpole.

4.1 One-loop Graviton Tadpole

Now we proceed to give some of the details of the calculation of the one-loop graviton tadpole in string theory described above. Our calculations are based on the functional method. We begin with a brief review of the latter, following [48]. As it turns out, an immediate difference with tadpole calculations on Euclidean orbifolds is in kinematics and in appropriate choice of polarization of vertex operators. We have also performed the same calculations in the oscillator formalism. It also turns out that there are some

interesting subtleties and differences with the standard discussion; detailed notes may be found in the appendix.

We should note that in the string computations, one usually performs a Wick rotation in both spacetime and worldsheet, necessary for formal convergence. If the target space is time-dependent, the standard techniques of analytic continuation may not be applicable.⁸ In the context of the $\mathbb{R}^{1,d}/\mathbb{Z}_2$ orbifold, the issue was already noted in [10]. In the present paper, we simply adopt the same strategy as in [10], namely we formally continue the worldsheet to Euclidean signature in the calculations to obtain an expression for the tadpole. As well, we will encounter zero-mode integrations whose values are defined by a spacetime Euclidean continuation. The result is apparently well-defined and in a later section, we search for a field theory formalism that is compatible with the low-energy limit. In that section, propagation on the orbifold will be essentially shown to be an identification of forward and backward propagation on the covering space $\mathbb{R}^{1,d}$. This may also explain why the formal analytic continuation prescription continues to work in the calculations of this section.

4.2 The Generating Functional on $\mathbb{R}^{1,d-1}$

Following [48], the generating functional is

$$Z[J] = \langle \exp\{i \int d^2w J_\mu(w, \bar{w}) X^\mu(w, \bar{w})\} \rangle . \quad (21)$$

In order to perform the functional integrals, we introduce a complete set eigenmodes X_I of the Laplacian ∇^2 on the toroidal worldsheet,

$$\begin{aligned} \nabla_w^2 X_I(w, \bar{w}) &= -\omega_I^2 X_I(w, \bar{w}) \quad , \\ \int d^2w X_I(w, \bar{w}) X_J(w, \bar{w}) &= \delta_{IJ} \end{aligned} \quad (22)$$

and expand the string embedding coordinates in the eigenmodes,

$$X^\mu(w, \bar{w}) = \sqrt{4\pi^2\alpha'} \sum_I x_I^\mu X_I(w, \bar{w}) . \quad (23)$$

We also denote

$$J_{\mu,I} = \sqrt{4\pi^2\alpha'} \int d^2w J_\mu(w, \bar{w}) X_I(w, \bar{w}) . \quad (24)$$

We then integrate out the expansion coefficients x_I^μ by completing the squares in the generating functional and performing the resulting Gaussian integrals. In particular, the

⁸See *e.g.* [50] for a proposal to modify the standard approach.

integrals will include zero mode contributions from x_0^μ . The result in d target space dimensions is

$$Z[J] = N[J_0] [\det'(-\nabla_w^2)]^{-d/2} \exp \left\{ -\frac{1}{2} \int d^2 w \int d^2 w' J(w) \cdot G'(w, w') \cdot J(w') \right\} , \quad (25)$$

where $N[J_0]$ is the zero mode contribution

$$N[J_0] = i(2\pi)^d \delta^{(d)}(J_0) , \quad (26)$$

(with i coming from the Wick rotation $x_I^0 \equiv ix_I^d$), the determinant factor is

$$\det'(-\nabla_w^2) \equiv \prod_{I \neq 0} \omega_I^2 , \quad (27)$$

and $G'(w, w')$ is the Green function

$$G'(w, w') = \sum_{I \neq 0} \frac{2\pi\alpha'}{\omega_I^2} X_I(w) X_I(w') . \quad (28)$$

The latter satisfies the differential equation

$$-\frac{1}{2\pi\alpha'} \nabla_w^2 G'(w, w') = g^{-1/2} \delta^{(2)}(w - w') - X_0^2 , \quad (29)$$

where X_0 is the zero mode of the Laplacian on the torus. The functional determinant (27) gives the torus partition function,

$$Z_{T^2}[0] = V_d [\alpha' X_0^2 \det'(-\nabla_w^2)]^{-d/2} \quad (30)$$

4.3 The Generating Functional on Orbifolds

Next we generalize this to the case of the orbifold. For comparison, we will consider two related types of orbifolds:

A) The Euclidean orbifold $\mathbb{R}^{1,d} \times \mathbb{R}^{25-d}/\mathbb{Z}_2$

B) The Lorentzian orbifold $\mathbb{R}^{1,d}/\mathbb{Z}_2 \times \mathbb{R}^{25-d}$.

To streamline the notation, we will denote the total number of orbifold directions in both cases as d_o . We split the coordinates X and the components of the source J into those along the orbifolded (o) and un-orbifolded (u) directions. The generating functional takes the form

$$Z[J] = \sum_{g=0}^1 \sum_{h=0}^1 \langle \exp \{ i \int J_o \cdot X_o + i \int J_u \cdot X_u \} \rangle_{gh} \quad (31)$$

including the sum over the untwisted ($g = 1$) and twisted ($g = 0$) sectors, with ($h = 0$) and without ($h = 1$) the \mathbb{Z}_2 reflection, for string oscillations in the orbifolded directions. We then again expand X^μ in the eigenmodes of ∇^2 , but now the eigenvalues and -modes will be different in the orbifolded directions for each sector, due to the different (anti)periodic boundary conditions. After integrating over the eigenmode coefficients, the functional takes the form

$$\begin{aligned} Z[J] &= \frac{N_u[J_0]}{N_u[0]} Z_u[0] \exp\left\{-\frac{1}{2} \int d^2w \int d^2w' J_u(w) \cdot J_u(w') G'(w, w')\right\} \\ &\times \sum_{gh} \frac{N_{o,gh}[J_0]}{N_{o,gh}[0]} Z_{o,(g,h)}[0] \exp\left\{-\frac{1}{2} \int d^2w \int d^2w' J_o(w) \cdot J_o(w') G'_{(g,h)}(w, w')\right\}. \end{aligned} \quad (32)$$

In the above, $N_u[J_0]$, $N_{o,(g,h)}[J_0]$ are the zero mode contributions (we have formally multiplied and divided by $N[0]$ recognizing that Z includes such a factor.) In the orbifolded directions, there are zero modes only in the untwisted sector without the \mathbb{Z}_2 reflection, and none in the other sectors because X satisfies an antiperiodic boundary condition in at least one of the toroidal worldsheet directions. Thus, for $J = k\delta^{(2)}(w - w')$,

$$\frac{N_{o,(1,1)}[J_0]}{N_{o,(1,1)}[0]} = \frac{1}{V_{d_o}} \delta^{(d_o)}(k) ; \quad N_{o,(g,h)}[k] = 1 \text{ for } (g, h) \neq (1, 1) . \quad (33)$$

The factors $Z_u[0]$, $Z_{o,(g,h)}$ are the partition function contributions from the directions transverse to and parallel with the orbifold, including the four untwisted and twisted (g, h) -sectors. Explicitly [10],

$$\begin{aligned} Z_{o,(1,1)} &= \frac{V_{d_o}}{2} \left| \frac{1}{\sqrt{\tau_2} \eta^2(\tau)} \right|^{d_o} \\ Z_{o,(g,h)} &= \left| \frac{\eta(\tau)}{\theta_{gh}(\tau)} \right|^{d_o}, \quad (g, h) \neq (1, 1) \end{aligned} \quad (34)$$

There are four different Green functions, corresponding to the different periodicities on the toroidal worldsheet. The doubly periodic one is [48]

$$G'_{(1,1)}(w, w') \equiv G'(w, w') = -\frac{\alpha'}{2} \ln \left| \theta_{11} \left(\frac{w - w'}{2\pi} \middle| \tau \right) \right|^2 + \pi \alpha' X_0^2 [\text{Im}(w - w')]^2, \quad (35)$$

and the other ones with at least one antiperiodic direction are

$$\begin{aligned}
G'_{(1,0)}(w, w') &= -\frac{\alpha'}{2} \ln \left| \frac{\theta_{11}(\frac{w-w'}{4\pi}|\tau)\theta_{10}(\frac{w-w'}{4\pi}|\tau)}{\theta_{00}(\frac{w-w'}{4\pi}|\tau)\theta_{01}(\frac{w-w'}{4\pi}|\tau)} \right|^2 \\
G'_{(0,1)}(w, w') &= -\frac{\alpha'}{2} \ln \left| \frac{\theta_{11}(\frac{w-w'}{4\pi}|\tau)\theta_{01}(\frac{w-w'}{4\pi}|\tau)}{\theta_{10}(\frac{w-w'}{4\pi}|\tau)\theta_{00}(\frac{w-w'}{4\pi}|\tau)} \right|^2 \\
G'_{(0,0)}(w, w') &= -\frac{\alpha'}{2} \ln \left| \frac{\theta_{11}(\frac{w-w'}{4\pi}|\tau)\theta_{00}(\frac{w-w'}{4\pi}|\tau)}{\theta_{01}(\frac{w-w'}{4\pi}|\tau)\theta_{10}(\frac{w-w'}{4\pi}|\tau)} \right|^2.
\end{aligned} \tag{36}$$

In n -point amplitudes, one also encounters self-contractions which require renormalization. A simple prescription is to subtract the divergent part $-\frac{\alpha'}{2} \ln |w - w'|^2$ from the Green functions and define their renormalized versions. The renormalized version of G'_{11} is [48]

$$G'_{(1,1),ren}(w, w) = -\frac{\alpha'}{2} \ln \left| \frac{\theta'_1(0|\tau)}{2\pi} \right|^2. \tag{37}$$

After some manipulations, the renormalized versions of the other Green functions also turn out to simplify considerably to the following simple forms:

$$G'_{(g,h),ren} = -\frac{\alpha'}{2} \ln |\theta_{gh}(0|\tau)|^4 \tag{38}$$

for $(g, h) \neq (1, 1)$.

4.4 One-loop Graviton Tadpole on the Orbifold

Consider then the one-loop graviton tadpole on the orbifold. The vertex operator for a state which is not projected out by the \mathbb{Z}_2 reflection must be symmetric under $X \rightarrow -X$, hence the relevant massless tadpole on the orbifold is

$$\begin{aligned}
&\langle V_{\mu\nu}(k_o, k_u) + V_{\mu\nu}(-k_o, k_u) \rangle \\
&= \frac{2g_{str}}{\alpha'} \langle \partial X^\mu \bar{\partial} X^\nu e^{ik_o \cdot X_o + ik_u \cdot X_u} + \partial X^\mu \bar{\partial} X^\nu e^{-ik_o \cdot X_o + ik_u \cdot X_u} \rangle
\end{aligned} \tag{39}$$

The momentum must satisfy the on-shell condition $k^2 = -m^2 = 0$. Now there are some immediate choices to be done where the Euclidean and Lorentzian orbifolds **A** and **B** differ. In string theory one often considers Euclidean orbifolds as a way of compactifying extra dimensions. Therefore one is usually interested in states which only propagate and carry polarization in the non-orbifolded noncompact directions, and the momentum and the polarization are chosen to be entirely transverse to the orbifold, with $k^2 = k_u^2 = -m^2$.

However, in the Lorentzian orbifold one must also include momentum components in orbifold directions in order to satisfy the on-shell condition. Furthermore, in the Lorentzian case, in order to compare with the quantum field theory calculation of Section 3, we choose the polarization to be along the orbifold directions⁹.

We evaluate the tadpole by first performing a point splitting and then functional differentiation of the generating functional,

$$\langle \partial X^\mu(w, \bar{w}) \bar{\partial} X^\nu(w, \bar{w}) e^{ikX(w, \bar{w})} \rangle = (-i)^2 \lim_{w_1, w_2 \rightarrow w} \partial_{w_1} \bar{\partial}_{w_2} \frac{\delta}{\delta J_\mu(w_1)} \frac{\delta}{\delta J_\nu(w_2)} \langle \exp \{ i \int d^2 w' J_\lambda(w') X^\lambda(w') \} \rangle, \quad (40)$$

evaluated at $J(w') = k \delta^{(2)}(w' - w)$. Before the functional differentiation, for the generating functional we substitute the integrated form (32). We will also substitute the on-shell condition $k^2 = 0$.

In the case where the polarizations are in the unorbifolded directions, the functional differentiation and the on-shell condition gives

$$\begin{aligned} \langle \partial X^\mu(w) \bar{\partial} X^\nu(w) e^{ikX} \rangle = & \frac{N_u[k]}{N_u[0]} Z_u[\tau] \lim_{w_1, w_2 \rightarrow w} [\eta^{\mu\nu} \partial_{w_1} \bar{\partial}_{w_2} G'(w_1, w_2) - k^\mu k^\nu \partial_{w_1} G'(w_1, w) \bar{\partial}_{w_2} G'(w_1, w)] \\ & \times \sum_{g, h} Z_{o, (g, h)}[\tau] \end{aligned} \quad (41)$$

whereas when the polarizations are in orbifolded directions, the corresponding result is

$$\begin{aligned} \langle \partial X^\mu(w) \bar{\partial} X^\nu(w) e^{ikX} \rangle = & \frac{N_u[k]}{N_u[0]} Z_u[\tau] \times \sum_{g, h} \frac{N_{o, (g, h)}[k]}{N_{o, (g, h)}[0]} Z_{o, (g, h)}[\tau] \\ & \lim_{w_1, w_2 \rightarrow w} [\eta^{\mu\nu} \partial_{w_1} \bar{\partial}_{w_2} G'_{(g, h)}(w_1, w_2) - k^\mu k^\nu \partial_{w_1} G'_{(g, h)}(w_1, w) \bar{\partial}_{w_2} G'_{(g, h)}(w_1, w)] \end{aligned} \quad (42)$$

In both cases, the Green function will need to be replaced by their renormalized versions. We can already see that the expressions are quite different. Let us simplify them further. First, we can use the equation (29) to simplify the double derivatives of the Green functions. First, since $G'(w_1, w_2) = G'(w_1 - w_2)$,

$$\partial_{w_1} \bar{\partial}_{w_2} G'(w_1, w_2) = -\partial_{w_1} \bar{\partial}_{w_1} G'(w_1, w_2). \quad (43)$$

⁹Another reason why this is the interesting case is to view the orbifold as a cosmological toy model. If one would make the model truly $d+1$ -dimensional, the extra dimensions would need to be compactified. The massless gravitons would carry polarization in the non-compact orbifold directions.

On the other hand, the equation (29) evaluates to

$$\partial_w \bar{\partial}_w G'(w, w') = -\pi \alpha' \delta^2(w - w') + \frac{\pi \alpha'}{2} X_0^2 . \quad (44)$$

The first term on the right hand side originates from the short distance divergence $G'(w_1, w_2) \sim \ln |w_1 - w_2|^2$ of the Green function, which we subtract off when we renormalize the Green functions. The latter then satisfy the equation

$$\partial_{w_1} \bar{\partial}_{w_2} G'_{ren}(w_1, w_2) = -\frac{\pi \alpha'}{2} X_0^2 . \quad (45)$$

Similar results hold for the renormalized Green functions $G'_{(g,h),ren}$. Since a zero mode X_0 exists only in the doubly periodic $(g, h) = (1, 1)$ sector, the double derivatives $\partial \bar{\partial} G'_{gh,ren}$ vanish in all the other three sectors.

Next, we examine the first derivatives of the renormalized Green functions. A short calculation shows that in all cases the Green functions have a short distance behavior of the type

$$\partial G'_{(g,h)}(w, w') \approx_{w \rightarrow w'} -\frac{\alpha'}{2} (w - w')^{-1} + C_{(g,h)}(\tau)(w - w') + \mathcal{O}((w - w')^3) \quad (46)$$

where $C_{(g,h)}(\tau)$ are rational functions of derivatives of theta functions at $(0|\tau)$. A similar formula is found for the antiholomorphic derivative $\bar{\partial} G'_{(g,h)}$. There is only one divergent term, due to the self-contraction of X with ∂X . The renormalization prescription again removes the divergent term, so the renormalized (derivatives of) Green function vanish in the limit $w \rightarrow w'$. Hence these terms will not contribute to the graviton tadpole.

Substituting all the normalization and partition function factors, the final results are

$$\langle V^{\mu\nu}(k) + V^{\mu\nu}(-k) \rangle_{1-loop} = -\frac{g_{str}}{4\pi\tau_2} \frac{\delta^{(d_u)}(k)}{V_u} Z_u[\tau] \times \sum_{g,h} \frac{N_{o,(g,h)}[k]}{N_{o,(g,h)}[0]} Z_{o,(g,h)}[\tau] \eta^{\mu\nu} . \quad (47)$$

for polarizations in the unorbifolded directions, and

$$\langle V^{\mu\nu}(k) + V^{\mu\nu}(-k) \rangle_{1-loop} = -\frac{g_{str}}{4\pi\tau_2} \frac{\delta^{(26)}(k)}{V_{26}} Z_u(\tau) Z_{o,(1,1)}[\tau] \eta^{\mu\nu} . \quad (48)$$

for polarizations in the orbifolded directions. By analogy, one would then expect this tadpole to vanish for the superstring.

Equation (47) is the standard result. In the case of the Lorentzian orbifold, we would like to think of spacetime as the orbifolded directions, while the unorbifolded directions are perhaps compactified. Thus in the Lorentzian orbifold, it is appropriate to consider (48). At first sight, this result looks rather surprising, as it is precisely the same as for a graviton in the usual $\mathbb{R}^{1,25}$ target space.

This is in direct conflict with the field theory calculation of the previous section, but we have already noted the problems of principal with that calculation. In the light of the string theory analysis, we must search for a field theory description that can be consistent with these results. A key observation is that the string calculation involved strings with k and $-k$, opposite spacelike momentum *and* energy.

5 Quantum Field Theory on $\mathbb{R}^{1,d}/\mathbb{Z}_2$ Revisited

Consider a point particle on the fundamental domain of $\mathbb{R}^{1,d}/\mathbb{Z}_2$. On the covering space, it corresponds to two particles: one with positive energy (propagating forward in time), and its image with negative energy (propagating backward in time) with opposite momentum (Fig. 7). In other words, for each particle with a momentum (k^0, \vec{k}) we must include its image with momentum $(-k^0, -\vec{k})$.

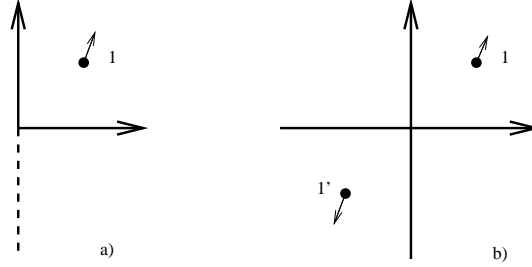


Figure 7: A point particle on the orbifold. a) depicts a single point particle on the fundamental domain, while b) depicts the point particle and its image on the covering space, moving towards the opposite time and space directions.

The situation is similar for strings on $\mathbb{R}^{1,d}/\mathbb{Z}_2$, as analyzed in [10]. The states in the untwisted sector which survive the \mathbb{Z}_2 projection are of the type

$$|\psi\rangle_S = (\alpha_{-n_1}^{\mu_1} \cdots \tilde{\alpha}_{-m_1}^{\nu_1} \cdots)_{S,A} (|0, k\rangle \pm |0, -k\rangle), \quad (49)$$

i.e. symmetrized combinations of string states with opposite pairs of center-of-mass momentum k . We conclude that in order to have a good description of quantum mechanics on the orbifold, we must start with pairs of states with opposite energy and momentum.

In quantum field theory in Minkowski space, 1-particle states in the Fock space are associated with positive energy,

$$|\omega_k, \vec{k}\rangle = a_k^\dagger |0\rangle \quad \text{with } k^0 = \omega_k > 0. \quad (50)$$

We should think of this as a projection of the Hilbert space containing both positive and negative energies. In a Euclidean orbifold, there would be an additional projection onto invariant states.

However, in order to formulate a quantum field theory on the Lorentzian orbifold covering space, we must also be able to include states with $k^0 = -\omega_k < 0$. In other words, what we need is a Fock space \mathcal{H} which involves sectors with both sign choices for the energy:

$$\begin{aligned}\mathcal{H}^+ &= \prod_{\vec{k}} \mathcal{H}_{\vec{k}}^+ \quad \text{with } k^0 = \omega_k > 0 \\ \mathcal{H}^- &= \prod_{\vec{k}} \mathcal{H}_{\vec{k}}^- \quad \text{with } k^0 = -\omega_k < 0 .\end{aligned}\tag{51}$$

The full Fock space is then the direct sum

$$\mathcal{H} = \mathcal{H}^+ \oplus \mathcal{H}^- .\tag{52}$$

This is an essential difference with usual Euclidean orbifolds. What survives on the orbifold QFT is the invariant Fock space. In the Euclidean case we can start directly with the usual Fock space \mathcal{H}^+ and project out the non-invariant states. However, in our case, in order to construct an invariant Fock space, we first need to extend the Fock space to include the \mathcal{H}^- sector. Next, to find the invariant states on the orbifold, we need to first implement the \mathbb{Z}_2 action as an isomorphism $\mathcal{H}^\pm \rightarrow \mathcal{H}^\mp$ which acts by flipping the sign of energy and momentum in the orbifolded directions. In particular, the usual vacuum $|0\rangle \in \mathcal{H}^+$ must map to a state in \mathcal{H}^- ; we will call it $|\tilde{0}\rangle$. We will later define it and other states in \mathcal{H}^- more precisely. The invariant Fock space is then

$$\mathcal{H}_{inv} = \mathcal{H}/\mathbb{Z}_2 .\tag{53}$$

Given this orbifold identification, it should be noted that there is no particular problem with the stability of the theory related to a negative energy sea.

Let us introduce two sets of annihilation and creation operators which at least provisionally commute with one another

$$[a_{\vec{k}}, \tilde{a}_{\vec{k}'}] = [a_{\vec{k}}, \tilde{a}_{\vec{k}'}^\dagger] = [a_{\vec{k}}^\dagger, \tilde{a}_{\vec{k}'}] = [a_{\vec{k}}^\dagger, \tilde{a}_{\vec{k}'}^\dagger] = 0 .\tag{54}$$

with

$$[a_{\vec{k}}, a_{\vec{k}'}^\dagger] = [\tilde{a}_{\vec{k}}, \tilde{a}_{\vec{k}'}^\dagger] = (2\pi)^d \delta^{(d)}(\vec{k} - \vec{k}') .\tag{55}$$

We envision that $a_{\vec{k}}$ destroys a particle with wavefunction $e^{-i\omega_{\vec{k}}t + i\vec{k}\cdot\vec{x}}$ which is positive energy and momentum with respect to the Killing vectors $E = i\partial_t$ and $P = -i\nabla$, whereas

$\tilde{a}_{\vec{k}}$ destroys a particle with wavefunction $e^{i\omega_{\vec{k}}t - i\vec{k}\cdot\vec{x}}$ which is negative energy and opposite momentum with respect to E and P . Let us then define a new vacuum $|\tilde{0}\rangle$ and 1-particle states:

$$\begin{aligned} |\tilde{0}\rangle & : \quad \tilde{a}_{\vec{k}}|\tilde{0}\rangle = 0 \\ |-\omega_{\vec{k}}, -\vec{k}\rangle & : \quad |-\omega_{\vec{k}}, -\vec{k}\rangle = \tilde{a}_{\vec{k}}^\dagger|\tilde{0}\rangle . \end{aligned} \quad (56)$$

We use the notation $|-\omega_{\vec{k}}, -\vec{k}\rangle$ to emphasize that these particles carry negative energy and opposite momentum. The above states are the images of the usual vacuum and 1-particle states of \mathcal{H}^+ under the \mathbb{Z}_2 isomorphism $\mathcal{H}^+ \rightarrow \mathcal{H}^-$, that we discussed earlier.

Next we need to take into account the identification and define \mathbb{Z}_2 invariant states on the fundamental domain; these are states in the invariant Fock space $\mathcal{H}_{inv} = (\mathcal{H}^+ \oplus \mathcal{H}^-)/\mathbb{Z}_2$. *E.g.* for 1-particle states we define

$$|\omega_{\vec{k}}, \vec{k}\rangle_{inv} = \frac{1}{\sqrt{2}} \begin{pmatrix} |+\omega_{\vec{k}}, +\vec{k}\rangle \\ |-\omega_{\vec{k}}, -\vec{k}\rangle \end{pmatrix} . \quad (57)$$

Invariant multiparticle states are constructed in an analogous fashion.

We propose that the natural energy operator on the orbifold is

$$H_{inv} = \sum_{\vec{k}} N_{\vec{k}} \omega_{\vec{k}} = \begin{pmatrix} \sum_{\vec{k}} \omega_{\vec{k}} a_{\vec{k}}^\dagger a_{\vec{k}} & \\ & \sum_{\vec{k}} \omega_{\vec{k}} \tilde{a}_{\vec{k}}^\dagger \tilde{a}_{\vec{k}} \end{pmatrix} = \begin{pmatrix} H^+ & \\ & H^- \end{pmatrix} . \quad (58)$$

The individual pieces H^\pm generate time translations in $\pm t$ directions. The orbifold identifies the two, hence on the covering space neither direction is preferred. So the theory on the covering space must start with a symmetric combination of the two Hamiltonians H^\pm . Including also the zero point energies in H^\pm (the \mathbb{Z}_2 invariance also extends to the zero energy contributions), we can then evaluate the vacuum energy on the orbifold,

$$\begin{aligned} {}_{inv}\langle 0|H_{inv}|0\rangle_{inv} &= \frac{1}{2}\langle 0|H^+|0\rangle + \frac{1}{2}\langle \tilde{0}|H^-|\tilde{0}\rangle \\ &= \frac{1}{2}\langle 0|\frac{1}{2}\sum_{\vec{k}}\omega_{\vec{k}}|0\rangle + \frac{1}{2}\langle \tilde{0}|\frac{1}{2}\sum_{\vec{k}}\omega_{\vec{k}}|\tilde{0}\rangle = \frac{1}{2}\sum_{\vec{k}}\omega_{\vec{k}} . \end{aligned} \quad (59)$$

This is the usual vacuum divergence.

The invariant Hamiltonian operator (58) must derive from an invariant stress tensor. Thinking of the latter as an operator, it will also reduce to components which act on the subspaces \mathcal{H}^\pm . In our notation, the invariant stress tensor should be written

$$T_{\mu\nu}^{inv}(t, \vec{x}) = \begin{pmatrix} T_{\mu\nu}^+(t, \vec{x}) & \\ & T_{\mu\nu}^-(-t, -\vec{x}) \end{pmatrix} \quad (60)$$

We would like to give a field theoretic description of such a calculation. Given the structure of the Fock space, it appears natural to describe the system using a pair of scalar fields which at least in some approximation do not interact with one another. Such doubling of the degrees of freedom seems to be a common occurrence in time-dependent backgrounds [50]. The novelty here is not so much this doubling, but the fact that we must deal carefully with the orbifold identification.

Finally, we comment on the number of degrees of freedom. Let us compare with $\mathbb{R} \times (\mathbb{R}^d/\mathbb{Z}_2)$ where \mathbb{R} is the time direction. In that case, the invariant Fock space has half as many degrees of freedom as the full Fock space. In $\mathbb{R}^{1,d}/\mathbb{Z}_2$, we first doubled the degrees of freedom and then projected out half of them, so the remaining number of states in $(\mathcal{H}^+ \oplus \mathcal{H}^-)/\mathbb{Z}_2$ is the same as in Minkowski space. However, recall the discussion after Fig. 2, on the freedom to choose the time direction on the fundamental domain. In order for the states not to propagate through the big crunch and continue on to the reversed time orientation, an additional projection would be needed. That projection would presumably again project out half of the states, so the remaining number would be in agreement with that in the Euclidean $\mathbb{R} \times (\mathbb{R}^d/\mathbb{Z}_2)$ orbifold. Essentially the projection should correspond to some sort of a boundary condition, presumably near the initial value surface. We don't know how to implement this precisely, but we will make some additional comments on this in the next section and in Section 6.

5.1 A Field Realization

There are of course other well known reasons to involve both positive and negative energy sectors in the formulation of QFT. One of them is QFT in curved spacetime, or other cases where we compare observers who are not related by proper orthochronous Lorentz transformations. The mode expansions of the field operator relevant for such observers are related by mixing of positive and negative energies. In the present case, the $\mathbb{R}^{1,d}/\mathbb{Z}_2$ spacetime is locally flat, but we want to identify (as opposed to compare) observers related by the time (and space) reflection, and identify the corresponding degrees of freedom.

Actually, a closely related starting point is QFT in flat spacetime but at finite temperature (FTQFT). The real-time formulation of FTQFT also leads to mixing between positive and negative energies. For inspiration, we shall review it briefly. The starting point in the path integral formulation of real-time FTQFT is the generating functional

$$Z[J] = \int \mathcal{D}\phi \exp \left\{ i \int_C d^4x [\mathcal{L}(\phi(x)) + J(x)\phi(x)] \right\} \quad (61)$$

where the time integral has been promoted to a contour integral along a complex time path C , starting from some initial time t_i and ending at a complex final time $t_i - i\beta$, where the

imaginary part is given by the inverse temperature $\beta = T^{-1}$ [52]. The functional integral is taken over all field configurations which satisfy the periodic boundary condition

$$\phi(t_i - i\beta, \vec{x}) = \phi(t_i, \vec{x}) . \quad (62)$$

One convenient choice of the complex time path consists of three segments, $C = C_1 \cup C_2 \cup C_3$, where C_1 runs along the real axis from t_i to some $t_f \gg t_i$, C_2 runs backwards along the time axis from t_f to t_i , and finally C_3 runs parallel to the imaginary axis from t_i to $t_i - i\beta$ (Fig. 8).

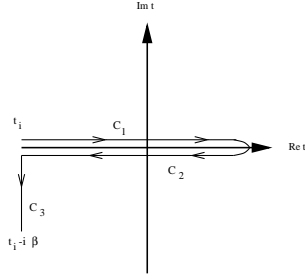


Figure 8: The time contour for FTQFT.

From the generating functional, one can calculate the thermal Green function

$$iD_C(x - x') = \langle T_C \phi(x) \phi(x') \rangle , \quad (63)$$

where time ordering has been promoted to path ordering T_C along the complex time path C . Equivalently, one can rewrite the thermal Green function in terms of a 3×3 matrix $(D^{rs})_{r,s=1,2,3}$ with components

$$D^{rs}(t - t') = D_C(t_r - t_s) \quad (64)$$

where $t = t_r$, $t' = t_s$ if $t \in C_r$ and $t' \in C_s$ along $C = C_1 \cup C_2 \cup C_3$. Furthermore, if one takes $t_i, t_f \rightarrow -\infty, +\infty$ in an appropriate manner, the contributions involving the segment C_3 decouple from the rest¹⁰. The matrix (D^{rs}) then reduces to a 2×2 matrix, but the temperature dependence remains, as the components depend on the distribution function of the thermal background. The contour C reduces to the Schwinger-Keldysh

¹⁰Strictly speaking, in order to take the energy eigenvalues correctly into account in the amplitudes of the interacting thermal theory, one needs to also take into account contributions from the vertical part of the contour [53]. However, this subtlety will not affect the remaining discussion in this paper. We thank Per Kraus for pointing this out.

contour [54, 55] $C_1 \cup C_2$. The propagator is reproduced by breaking up the field ϕ and the source J into two-component vectors,

$$\begin{aligned}\phi &= (\phi_1, \phi_2) \text{ with } \phi_r(x) = \phi(t_r, \vec{x}), \ t_r \in C_r \\ J &= (J_1, J_2) \text{ with } J_r(x) = J(t_r, \vec{x}), \ t_r \in C_r.\end{aligned}\tag{65}$$

The generating functional (61) then reduces to a form

$$Z[J_1, J_2] = \int \mathcal{D}\phi_1 \mathcal{D}\phi_2 \exp \left\{ i \int_{-\infty}^{\infty} d^4x [\phi_r(D^{-1})^{rs}\phi_s + \mathcal{L}_{int}(\phi_1) - \mathcal{L}_{int}(\phi_2) + J_r\phi_r] \right\}\tag{66}$$

where \mathcal{L}_{int} is the interaction part of the Lagrangian. In particular, the diagonal components of the 2×2 propagator D^{rs} have the momentum space representation

$$\begin{aligned}iD^{11}(k) &= \frac{i}{k^2 - m^2 + i\epsilon} + 2\pi\delta(k^2 - m^2)n_T(k_0) \\ iD^{22}(k) &= \frac{-i}{k^2 - m^2 - i\epsilon} + 2\pi\delta(k^2 - m^2)n_T(k_0)\end{aligned}\tag{67}$$

where $n_T(k_0)$ is essentially the thermal distribution function. It is then evident that in addition to the physical field ϕ_1 , the theory contains another degree of freedom ϕ_2 , called the thermal ghost, which propagates backwards in time. The two fields $\phi_{1,2}$ are coupled together only by the off-diagonal elements $D^{12,21}$ of the propagator. One is interested in correlation functions of ϕ_1 only. Furthermore, it can be shown that in the zero temperature limit $\beta \rightarrow \infty$ the off-diagonal elements of the propagator vanish, $D^{12,21} \rightarrow 0$, so that the thermal ghost decouples from the physical degree of freedom. Hence at zero temperature one can ignore the thermal ghost and the theory reduces back to the usual form involving only the physical degree of freedom. But at any finite T , both fields make physical contributions.

The orbifold case. In the above example, the Fock spaces associated with the physical field and thermal ghost are the positive and negative energy sectors \mathcal{H}^+ and \mathcal{H}^- . At zero temperature, before removing the thermal ghost, the generating functional (66) is symmetric under \mathbb{Z}_2 reflection which reverses the direction of time. This is precisely what we need as a starting point for QFT on the covering space of $\mathbb{R}^{1,d}/\mathbb{Z}_2$. We will also start with a path integral involving the Schwinger-Keldysh contour as the complex time path. Then, as before, we break up the field ϕ as a two-component vector $\phi = (\phi_+, \phi_-)$ where ϕ_+ and ϕ_- involve times at the forward and backward running segments of the Schwinger-Keldysh contour. The path integral can then be rewritten as

$$Z = \int \mathcal{D}\phi_+ \mathcal{D}\phi_- \exp \left\{ i \int_{-\infty}^{\infty} dt \int d^d\vec{x} [\mathcal{L}(\phi_+) - \mathcal{L}(\phi_-)] \right\},\tag{68}$$

where \mathcal{L} is the (for example) scalar field Lagrangian

$$\mathcal{L}(\phi) = \frac{1}{2}(\partial\phi)^2 - \frac{1}{2}m^2\phi^2 - V_{int}(\phi) . \quad (69)$$

We have made physical input here by the choice of propagator for $\{\phi_+, \phi_-\}$. On the covering space, our picture is that the field ϕ_+ propagates forward and its copy field ϕ_- propagates backward in time, decoupled from each other for $t \neq 0$. Hence the propagator is diagonal in ϕ_+, ϕ_- . We then choose the $t = 0$ hypersurface as the time slice where we define initial conditions¹¹. More precisely, we could consider the time evolution of ϕ_+ from $t < 0$ up to a specified profile at $t = 0$ and then forward to $t > 0$, and the reverse for ϕ_- . The orbifold identification then calls us to identify the fields and time evolutions (elaborated further below). However, note first a subtlety in defining the initial condition. At $t = 0$ the orbifold identification is $(0, x) \sim (0, -x)$, hence the profiles of ϕ_+ and ϕ_- must become symmetric at $t = 0$. The most natural initial condition is to set the profiles to be equal at $t = 0$. Thus our initial condition is

$$x > 0 : \quad \phi_+(0, x) = \phi_+(0, -x) = \phi_-(0, x) = \phi_-(0, -x) = \phi_0(x) \quad (70)$$

where $\phi_0(x)$ is the specified initial profile on $x > 0$. This can be satisfied as follows. Decompose the fields ϕ_{\pm} into symmetric and antisymmetric parts under $x \mapsto -x$:

$$\begin{aligned} \phi_{\pm}(t, x) &= \phi_{\pm,S}(t, x) + \phi_{\pm,A}(t, x) , \\ \phi_{\pm,S}(t, x) &= \frac{1}{2}(\phi_{\pm}(t, x) + \phi_{\pm}(t, -x)) \\ \phi_{\pm,A}(t, x) &= \frac{1}{2}(\phi_{\pm}(t, x) - \phi_{\pm}(t, -x)) . \end{aligned} \quad (71)$$

The initial condition can be satisfied if the antisymmetric parts $\phi_{\pm,A}$ decay to strictly zero sufficiently rapidly as $t \rightarrow 0$ (and the symmetric parts become equal). There is a subtlety here in what exactly should be meant by “sufficiently rapid,” and we will comment on it further below.

While the above serves as a starting point for our construction of the theory on the covering space, we must also take into account the identification which is part of the orbifold construction. We already discussed this in the context of Fock space states, and can now do it more explicitly. Let us leave the path integral formalism and return back to the canonical quantization prescription. In the remainder of this section, we focus only on the free field part of the Lagrangian. This is sufficient for the construction of the invariant Fock space, and for the improved invariant version of the back-reaction calculation which

¹¹Hence we are choosing the fundamental domain to be that of Figures 2 b) and 4. While this is the most convenient choice for our QFT construction, other choices would also be possible.

will replace that of Section 3. We will present a tentative discussion of interacting theory and the S-matrix in Section 6.

First, we quantize the field operators ϕ_{\pm} . While ϕ_+ has the standard free field mode expansion

$$\phi_+(t, \vec{x}) = \int \frac{d^d \vec{k}}{(2\pi)^d} \frac{1}{\sqrt{2\omega_k}} \left\{ a_{\vec{k}} e^{-i\omega_{\vec{k}} t + i\vec{k} \cdot \vec{x}} + a_{\vec{k}}^\dagger e^{+i\omega_{\vec{k}} t - i\vec{k} \cdot \vec{x}} \right\} , \quad (72)$$

for the operator ϕ_- we write the mode expansion as

$$\phi_-(t, \vec{x}) = \int \frac{d^d \vec{k}}{(2\pi)^d} \frac{1}{\sqrt{2\omega_k}} \left\{ \tilde{a}_{\vec{k}} e^{+i\omega_{\vec{k}} t - i\vec{k} \cdot \vec{x}} + \tilde{a}_{\vec{k}}^\dagger e^{-i\omega_{\vec{k}} t + i\vec{k} \cdot \vec{x}} \right\} . \quad (73)$$

The initial condition at $t = 0$ and the required rapid decay of the antisymmetric parts of ϕ_{\pm} create subtleties, but the above mode expansions are valid sufficiently far from the $t = 0$ slice. Since the field ϕ_- is decoupled from ϕ_+ , violations of causality do not arise.

We can now present an improved (completely \mathbb{Z}_2 invariant) version of the calculation of the vacuum expectation value of the stress tensor. Since the initial condition creates subtleties near $t = 0$, we first assume $|t| > 0$ so that we can trust the mode expansions. Then, simply

$$\begin{aligned} {}_{inv}\langle 0 | T_{\mu\nu}^{inv}(x) | 0 \rangle_{inv} &= \frac{1}{2} (\langle 0 |, \langle \tilde{0} |) \begin{pmatrix} T_{\mu\nu}^+(x) & \\ & T_{\mu\nu}^-(-x) \end{pmatrix} \begin{pmatrix} |0\rangle \\ |\tilde{0}\rangle \end{pmatrix} \\ &= \lim_{x' \rightarrow x} \frac{1}{2} \left\{ \langle 0 | \partial_\mu \phi_+(x) \partial_\nu \phi_+(x') | 0 \rangle + \langle \tilde{0} | \partial_\mu \phi_-(-x) \partial_\nu \phi_-(-x') | \tilde{0} \rangle \right\} \\ &= \lim_{x' \rightarrow x} \frac{1}{2} \left\{ \frac{1}{(x - x')^2} + \frac{1}{(x - x')^2} \right\} = \lim_{x' \rightarrow x} \frac{1}{(x - x')^2} . \end{aligned} \quad (74)$$

This is again just the usual vacuum divergence. The renormalized expectation value of T_{inv} would then be equal to zero. There are two main differences with the previous calculation of Section 2: i) Everything is \mathbb{Z}_2 invariant, including the vacuum state. ii) Essentially, $\phi(-u)$ is now replaced by ϕ_- . But ϕ_{\pm} are decoupled, so there are no “ $\langle 0 | \phi_+ \phi_- | 0 \rangle$ ” cross contractions, as were depicted in Fig. 6.

Near the initial slice $t = 0$ the situation is more subtle. As noted previously, the antisymmetric part of the fields must die off sufficiently rapidly. Such behavior will alter the mode expansion of the fields. If we insist on trusting the mode expansion everywhere such that $t \neq 0$, then we must switch off the antisymmetric parts abruptly with step functions:

$$\phi_{+,A}(t, \vec{x}) = (1 - \theta(t)) f_+(\vec{x}) ; \quad \phi_{-,A}(-t, -\vec{x}) = (1 - \theta(-t)) f_-(-\vec{x}) , \quad (75)$$

separating out the time dependence. But then the tt component of the invariant stress tensor will have a $\delta^2(t)$ singularity and the tx^i components a $\delta(t)$ singularity at the initial

slice $t = 0$. However, if we interpret the $\mathbb{R}^{1,d}/\mathbb{Z}_2$ orbifold as a toy model of cosmology, then the $t = 0$ slice plays the role of the initial singularity. Having a divergent stress tensor at the $t = 0$ slice is then natural in such a cosmological interpretation — it could represent the necessity for appropriate boundary conditions.

However, it is not clear how seriously we should take the initial condition leading to the divergence, as we did not derive it from a low-energy limit of a string calculation. The low-energy limit the first quantized string analysis of Section 4 yields no such thing. Moreover, the existence of the twisted sector, localized at the orbifold singularity, is related to more involved question of whether there is a blow-up mode and whether the singular geometry really is the actual geometry on which to consider the QFT. We leave these questions for future work. The main point that we would like to stress here is that the stress tensor does not have a divergence from back reaction as the naive analysis would have suggested. That kind of a singularity would have been a signal of a more serious instability.

Note also that although the covering space first appeared to have CTCs everywhere, in the reformulation of QFT it is also apparent that nothing actually propagates along a CTC. Instead of a single quantum propagating around and around in a CTC, there is a quantum and its copy which propagate in opposite directions. More precisely¹², if a particle on the covering space starts out at $t < 0$ with a future-directed tangent vector, when it reaches the image point at $t > 0$, its future-directed tangent vector corresponds to a past-directed tangent vector at the starting point. So the future-going particle at $t > 0$ is then identified with a past-going particle at the initial point $t < 0$. Thus the particle cannot loop around the CTC on the covering space, since its initial condition is not repeated. What the chronology protection conjecture is meant to forbid is closed paths that a particle can follow and return to its initial condition, this is the essence of a time-machine. This is not possible in the reformulated QFT, therefore it is not a surprise that the instabilities associated with looping around CTCs also do not arise.

6 Time Evolution and Local S-matrix on the Fundamental Domain

In all previous discussions, we limited the analysis to what corresponds to free field theory in the low-energy limit. What then of the interacting theory? Given that the orbifold is globally time-nonorientable, is there any way of defining S-matrices at least locally, for example away from the $t = 0$ axis in the above choice of the fundamental domain? A full analysis of these questions is beyond the scope of the present paper, but we can make

¹²We thank Simon Ross for the following elegant argument.

some tentative comments and proposals. Let us first illustrate the problem with a simple figure. Figure 9 depicts a point particle and its image propagating in opposite time and

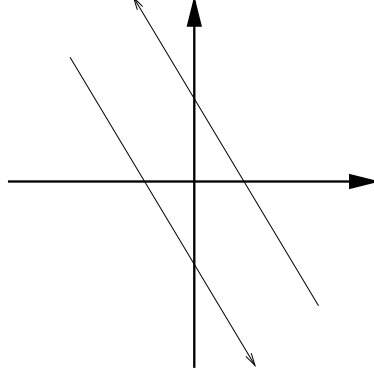


Figure 9: Example of a point particle and its image propagating on the covering space.

space directions on the covering space. As discussed in Section 5, both trajectories will be identified by the \mathbb{Z}_2 reflection, resulting in a single trajectory for a point particle on the fundamental domain. The details depend on the choice of the fundamental domain.

Consider first choosing the right half-space as the fundamental domain, and drawing the corresponding "pocket", as depicted in Figure 10 (see also Figs. 2(a) and 3). Alternatively, we can choose the upper half-space as the fundamental domain, and identify the negative x -axis with the positive x -axis. The result is depicted in Figure 11 (see also Figs. 2(b) and 4).

As discussed in Section 2, a possible choice for the time-arrow on the fundamental domain of Figure 10 is to let it point from the lower right quadrant to the upper right quadrant, while becoming ambiguous on the $x = 0$ axis. On the pocket, time would thus flow down the front fold and continue upwards on the rear fold. Similarly, on the fundamental domain of Figure 11 one can choose the arrow of time to point upwards on the upper half-space, with the $t = 0$ axis as the origin of time. On the pocket, time would then flow upwards on both sides of the fold. However, then the trajectories depicted on the figures would seem to violate causality. On Figure 10, if we choose a constant time slice far up on the front fold, the trajectory will cross it twice. First it crosses the slice on its way down along the front fold, then it continues to the other side but returns back to the front slice and crosses the slice again. On Figure 11, the trajectory would propagate first backwards in time towards $t = 0$, then propagate forward in time on the rear fold and again on the front fold. Both interpretations are troublesome.

However, we can improve the situation a bit. In Section 5, we identified forward time evolution of a particle with backward time evolution of its image on the covering space.

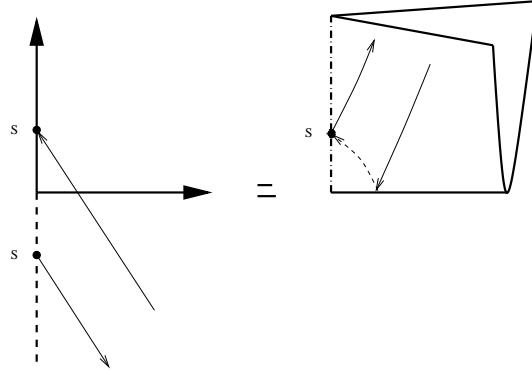


Figure 10: Point particle propagating on the fundamental domain. The left part of the figure depicts the fundamental domain, with the dashed negative time axis ($x = 0$) identified with the positive time axis. For example, the points S marked with a black dot are identified. The identification results in the pocket shown on the right. The time orientation breaks down on the time axis. The part of the trajectory drawn with solid lines depicts propagation on the front fold of the pocket, while the dashed line depicts propagation on the rear fold. The point S is on dotted-dashed line, where the time direction becomes ill-defined.

We start the forward evolution from $t = -\infty$ and the backward evolution from $t = \infty$. The time evolution continues without problems until we reach the dividing line between the two half-spaces, depending on the choice of the fundamental domain. That is, if we choose the right half-space as the fundamental domain, we can follow the time evolution until the particle and its image reach $x = 0$. If we choose the upper half-space as the fundamental domain, the time evolution can be followed up to $t = 0$. Similarly, just after crossing the dividing line, we can again follow the time evolution onwards. For example, in the latter case we can continue from $t = 0 + \epsilon$ the forward time evolution to $t = \infty$ and backward evolution to $t = -\infty$. The problem is if and how it is possible to continue the evolution across the dividing line.

If we choose the upper half-space as the fundamental domain, it is simple to give a more formal definition. In the Heisenberg picture we define the invariant time evolution

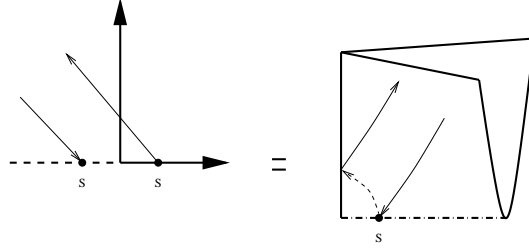


Figure 11: Point particle propagating on the fundamental domain. On the left figure, the points marked with S are identified. On the right figure, the solid lines depict propagation on the front fold of the pocket, the dashed line depicts propagation on the rear fold. The point marked with S is on the dotted-dashed line, where the time direction becomes ill-defined.

operator from t_0 to $t_1 > t_0$ on the covering space to be

$$\begin{aligned}
 U_{inv}(t_0, t_1) &= T \left\{ \exp \left[-i \int_{t_0}^{t_1} dt H_{inv}(t) \right] \right\} \\
 &= \begin{pmatrix} T \{ \exp[-i \int_{t_0}^{t_1} dt H^+] \} & 0 \\ 0 & \tilde{T} \{ \exp[-i \int_{-t_0}^{-t_1} dt H^-] \} \end{pmatrix} \\
 &= \begin{pmatrix} U^+(t_0, t_1) & 0 \\ 0 & U^-(-t_0, -t_1) \end{pmatrix}, \tag{76}
 \end{aligned}$$

where \tilde{T} denotes anti-time ordering. This is unambiguously defined if both $t_0, t_1 < 0$ or both $t_0, t_1 > 0$. Problems arise when $t_0 < 0$ and $t_1 > 0$.

Let us see what this means for the point particles in the figures. In Figure 9, we launch the particle and its image from $t = -\infty$ and $t = +\infty$, and then propagate them using $U(-\infty, t)$ towards the x -axis, *i.e.* up to $t = 0 - \epsilon$. This gives the lower half and the upper half of the forward and backward trajectories of Fig. 9. They are identified on the fundamental domain, so this gives the “downward” trajectory on the left part in Figure 11 all the way to the marked point S, and the downward trajectory to the point S on the front fold of the pocket in Figure 11. Similarly, we could propagate forward and backward from $t = 0 + \epsilon$, giving the other halves of the trajectories in Figure 9. In Figure 11, the resulting trajectory is the “upward” one on the left diagram, and the upward trajectory starting on the rear fold and continuing to the front fold of the pocket.

To summarize, on the fundamental domain (the pocket), we can either choose the time to point downwards, corresponding to Figure 2 b) with the arrows reversed, and consider time evolution up to a “big crunch” at $t = 0$, or choose the time to point upwards and consider time evolution forward from a “big bang”. The latter corresponds

to Figure 2 b). Either way, the evolution breaks down at $t = 0$. But that is also the point where from Section 5 we know the stress tensor to diverge¹³. The choice could be interpreted as the additional projection on degrees of freedom, discussed in section 5., with the remaining number of states being one half of those in Minkowski space, in analogue with the Euclidean \mathbb{Z}_2 orbifold.

Consider then an interacting field theory. We could adopt the interaction picture, and define the time evolution operator as

$$U_{I,inv}(t_0, t_1) = \begin{pmatrix} T\{\exp[+i \int_{t_0}^{t_1} dt d^d \vec{x} \mathcal{L}_I(\phi_+(t, \vec{x}))]\} & 0 \\ 0 & T\{\exp[-i \int_{t_0}^{t_1} dt' d^d \vec{x} \mathcal{L}_I(\phi_-(t', \vec{x}))]\} \end{pmatrix} \quad (77)$$

where \mathcal{L}_I is the interaction part of the Lagrangian. We could consider this as the local S-matrix. Hence, as long as we stay away from the singular $t = 0$ hypersurface, the S-matrix has the same properties as that of an ordinary field theory on Minkowski space.

Acknowledgment

We would like to thank Vijay Balasubramanian, Fawad Hassan, and Asad Naqvi for the collaboration which lead us to this investigation, and many discussions on the interpretational issues. We also thank Per Kraus for helpful discussions and useful encouragement, and Simon Ross for useful discussions on time-nonorientability and time travel. EK-V was in part supported by the Academy of Finland, and thanks the University of California at Los Angeles and University of Pennsylvania for hospitality at different stages of this work. RGL was supported by US DOE under contract DE-FG02-91ER40677 and thanks the Helsinki Institute of Physics for hospitality. ES would like to thank A. Lawrence, S. Kachru, A. Knutson and R. Bryant for helpful conversations. Finally, we thank the Aspen Center for Physics for hospitality, and the participants of the workshop "Time and String Theory" for useful discussions, as we were re-editing this paper.

A Appendix

In this appendix, we will provide the details of complementary calculations using oscillator methods. There are several subtleties that are not regularly seen in the usual backgrounds. We will use the notation where \tilde{k} is the image of k under the orbifold.

$$\tilde{k}_o = -k_o \quad (78)$$

$$\tilde{k}_u = +k_u \quad (79)$$

¹³Similar analysis, based on the other two choices of the fundamental domain, Figure 2 a) and c), are also possible. Then the time evolution would break down at $x = 0$ (a) or at null cone (c).

We want to evaluate

$$T(\tau) = \frac{1}{2} \text{tr}_{U+T} \left[(1 + \hat{g}) \int d^2 z V(z, \bar{z}) q^{L_o - a} \bar{q}^{\tilde{L}_o - \tilde{a}} \right] \quad (80)$$

It is important to note that in this formalism, obtained by sewing the cylinder into a torus, there are zero modes in the U sectors of the trace, but not in the twisted T sectors. The massless vertex operator is of the form

$$V(z, \bar{z}) = \frac{2g_{str}}{\alpha'} : \partial X^\mu \bar{\partial} X^\nu \frac{1}{2} \left(e^{ik \cdot X(z, \bar{z})} + e^{i\tilde{k} \cdot X(z, \bar{z})} \right) : \quad (81)$$

The non-zero mode portion of this expression can be evaluated using coherent state methods. For each oscillator α_n^μ ($n > 0$) we introduce a coherent-state basis $|\rho_{n,\mu}\rangle$ and write the trace as a ρ -integral. If the ∂X^μ does not contribute an oscillator, we find (for each $n > 0$ and μ)

$$\int \frac{d^2 \rho}{\pi} e^{-|\rho|^2} e^{\alpha' k_\mu^2 / 4n} (\rho | e^{\sqrt{\alpha'/2} k_\mu \alpha_{-n}^\mu z^n / n} e^{-\sqrt{\alpha'/2} k_\mu \alpha_n^\mu z^{-n} / n} | q^n \rho) \quad (82)$$

for the 1-insertion, while for the \hat{g} -insertion, we get

$$\int \frac{d^2 \rho}{\pi} e^{-|\rho|^2} e^{\alpha' k_\mu^2 / 4n} (\rho | e^{\sqrt{\alpha'/2} \tilde{k}_\mu \alpha_{-n}^\mu z^n / n} e^{-\sqrt{\alpha'/2} \tilde{k}_\mu \alpha_n^\mu z^{-n} / n} | - q^n \rho) \quad (83)$$

This is a standard integral whose evaluation can be found in [51]. The result is

$$\frac{1}{1 \mp q^n} e^{\mp \alpha' k_\mu k^\mu \frac{q^n}{2n(1 \mp q^n)}} \quad (84)$$

again for each $n > 0$ and μ . For the $\tilde{\alpha}$ oscillators, we will get the same result, with q replaced by \bar{q} . Now by simple re-ordering of sums and appropriate¹⁴ renormalization, we may compute:

$$\prod_{n \in \mathbb{Z}^+} e^{\frac{1}{n} \frac{q^n}{1+q^n}} = \frac{\theta_2(\tau)}{q^{1/8}}, \quad \prod_{n \in \mathbb{Z}^+ - 1/2} e^{\frac{1}{n} \frac{q^n}{\pm 1 + q^n}} = \theta_{3,4}(\tau) \quad (85)$$

On the other hand, the ∂X^μ might contribute an oscillator. Then, we have a new matrix element

$$\sum_{m>0} \int \frac{d^2 \rho}{\pi} e^{-|\rho|^2} (\rho | e^{\sqrt{\alpha'/2} k_\mu \alpha_{-n}^\mu z^n / n} [z^{-m-1} \alpha_m^\mu + z^{m-1} \alpha_{-m}^\mu] e^{-\sqrt{\alpha'/2} k_\mu \alpha_n^\mu z^{-n} / n} | q^n \rho) \quad (86)$$

¹⁴In particular, there is a factor of 2 which must be absorbed by the (implicit) regulator in the first equation. This can be seen, for example, as a requirement of modular invariance.

When $m = n$, we find, recalling that $[\alpha_m, e^{a\alpha-m}] = ma e^{a\alpha-m}$ and $|\rho_n\rangle = e^{\rho\alpha-n/\sqrt{n}}|0\rangle$

$$\frac{\sqrt{m}}{z} \int \frac{d^2\rho}{\pi} e^{-|\rho|^2} [z^{-m} q^m \rho + z^m \bar{\rho}] (\rho | e^{k_\mu \alpha_n^\mu z^n/n} e^{-k_\mu \alpha_n^\mu z^{-n}/n} | q^n \rho) \quad (87)$$

$$= \frac{\sqrt{m}}{z} \int \frac{d^2\rho}{\pi} e^{-(1-q^m)|\rho|^2} [z^{-m} q^m \rho + z^m \bar{\rho}] e^{k_\mu (z^m \bar{\rho} - z^{-m} q^m \rho)/\sqrt{m}} \quad (88)$$

It is straightforward to show that this vanishes. Thus only the zero mode part of the ∂X^μ factors contribute. As a corollary then, only the untwisted sector will contribute to the massless tadpole in the Lorentzian orbifold.

It remains to evaluate the zero modes. These are

$$\begin{aligned} U, 1 : \quad & \prod \int \frac{dp}{2\pi} \langle p | \hat{P}^\mu \hat{P}^\nu e^{-\pi\alpha'\tau_2 \hat{P}^2} e^{(\alpha'/2)k\hat{P} \ln|z|^2} | p+k \rangle |z|^{-\alpha'k_o^2/2} = \frac{\eta^{\mu\nu}}{2\pi\alpha'\tau_2} \prod_o \frac{\delta(\sqrt{\alpha'}k_o)}{\sqrt{\tau_2}} \\ U, \hat{g} : \quad & \prod \int \frac{dp}{2\pi} \langle \tilde{p} | \hat{P}^\mu \hat{P}^\nu e^{-\pi\alpha'\tau_2 \hat{P}^2} e^{(\alpha'/2)k\hat{P} \ln|z|^2} | p+k \rangle |z|^{-\alpha'k_o^2/2} = \\ & = \prod_o \frac{e^{-\pi\tau_2\alpha'k_o^2/4}}{2} \times \begin{cases} k_\mu k_\nu/4 & \mu, \nu \in o \\ \frac{1}{2\pi\alpha'\tau_2} & \mu = \nu \in u \end{cases} \end{aligned} \quad (89)$$

each times a factor $-(\frac{\alpha'}{2})^2 \frac{1}{|z|^2} \prod_u \frac{\delta(\sqrt{\alpha'}k_u)}{\sqrt{\tau_2}}$. In the first case, this is multiplied by $X_{1,1} = |\eta(\tau)|^{-24}$, while in the second, we have $X_{1,0} = \prod_n |q^{-1}(1-q^n)^{d-23}(1+q^n)^{-(d+1)}|^2$. Thus, if we go on-shell, we get

$$T_0^{\mu\nu} = - \left(\frac{g_{str}\alpha'}{2} \right) \prod_u \frac{\delta(\sqrt{\alpha'}k_u)}{\sqrt{\tau_2}} \frac{\eta^{\mu\nu}}{2\pi\alpha'} \left(\prod_o \frac{\delta(\sqrt{\alpha'}k_o)}{\sqrt{\tau_2}} X_{1,1} + 2^{-(d+1)} \sum_{(g,h) \neq (1,1)} X_{g,h} \right) \quad (90)$$

if μ, ν are in the unorbifolded directions, while if they are in the orbifolded directions

$$T_0^{\mu\nu} = - \left(\frac{g_{str}\alpha'}{2} \right) \prod_u \frac{\delta(\sqrt{\alpha'}k_u)}{\sqrt{\tau_2}} \left(\frac{\eta^{\mu\nu}}{2\pi\alpha'} \prod_o \frac{\delta(\sqrt{\alpha'}k_o)}{\sqrt{\tau_2}} X_{1,1} + \frac{k_\mu k_\nu}{4} 2^{-(d+1)} X_{1,0} \right) \quad (91)$$

This result is not modular invariant. However there is an ordering ambiguity¹⁵ in zero modes from the (U, \hat{g}) sector that we have not taken into account. To see the problem, suppose we write the vertex operator as

$$V = \alpha \partial X^\mu \bar{\partial} X^\nu e^{ik \cdot X} + \beta \partial X^\mu e^{ik \cdot X} \bar{\partial} X^\nu + e^{ik \cdot X} \partial X^\mu \bar{\partial} X^\nu \quad (92)$$

Then, the $k_\mu k_\nu/4$ in eq. (91) is multiplied by $\alpha + 2\beta + \gamma$. There is a modular invariant choice ($\alpha + \beta + \gamma = 1$, $\beta = -1$) for which the kk terms cancel. (There is no other effect of

¹⁵This ambiguity does not appear for Euclidean orbifolds.

this ordering issue.) We then obtain (In the notation of Section 4, $X_{1,1} = \frac{\tau_2^{12}}{V_{26}} Z_{o,(1,1)} Z_u$)

$$T_0^{\mu\nu} = - \left(\frac{g_{str}}{4\pi\tau_2} \right) \eta^{\mu\nu} \frac{\delta^{(26)}(k)}{V_{26}} Z_{o,(1,1)}[\tau] Z_u[\tau] \quad (93)$$

(for μ, ν in the orbifold directions). This result agrees with the result in Section 4 for the case of the Lorentzian orbifold.

References

- [1] G. T. Horowitz and A. R. Steif, “*Singular string solutions with nonsingular initial data*,” *Phys. Lett.* **B258** (1991) 91–96.
- [2] C. R. Nappi and E. Witten, “*A Closed, expanding universe in string theory*,” *Phys. Lett.* **B293** (1992) 309–314, hep-th/9206078.
- [3] C. Kounnas and D. Lust, “*Cosmological string backgrounds from gauged WZW models*,” *Phys. Lett.* **B289** (1992) 56–60, hep-th/9205046.
- [4] E. Kiritsis, “*Duality symmetries and topology change in string theory*,” hep-th/9309064.
- [5] E. J. Martinec, “*Space - like singularities and string theory*,” *Class. Quant. Grav.* **12** (1995) 941–950, hep-th/9412074.
- [6] A. E. Lawrence and E. J. Martinec, “*String field theory in curved spacetime and the resolution of spacelike singularities*,” *Class. Quant. Grav.* **13** (1996) 63–96, hep-th/9509149.
- [7] J. Khoury, B. A. Ovrut, N. Seiberg, P. J. Steinhardt, and N. Turok, “*From big crunch to big bang*,” *Phys. Rev.* **D65** (2002) 086007, hep-th/0108187.
- [8] N. Seiberg, “*From big crunch to big bang - is it possible?*,” hep-th/0201039.
- [9] G. Veneziano, “*String cosmology: The pre-big bang scenario*,” hep-th/0002094.
- [10] V. Balasubramanian, S. F. Hassan, E. Keski-Vakkuri, and A. Naqvi, “*A space-time orbifold: a toy model for a cosmological singularity*,” *Phys. Rev.* **D67** (2003) 026003, hep-th/0202187.
- [11] N. A. Nekrasov, “*Milne universe, tachyons, and quantum group*,” hep-th/0203112.

- [12] L. Cornalba and M. S. Costa, “*A New Cosmological Scenario in String Theory*,” *Phys. Rev.* **D66** (2002) 066001, hep-th/0203031.
- [13] J. Simon, “*The geometry of null rotation identifications*,” *JHEP* **06** (2002) 001, hep-th/0203201.
- [14] H. Liu, G. Moore, and N. Seiberg, “*Strings in a time-dependent orbifold*,” *JHEP* **06** (2002) 045, hep-th/0204168.
- [15] H. Liu, G. Moore, and N. Seiberg, “*Strings in time-dependent orbifolds*,” *JHEP* **10** (2002) 031, hep-th/0206182.
- [16] G. T. Horowitz and J. Polchinski, “*Instability of spacelike and null orbifold singularities*,” *Phys. Rev.* **D66** (2002) 103512, hep-th/0206228.
- [17] A. Lawrence, “*On the instability of 3D null singularities*,” *JHEP* **11** (2002) 019, hep-th/0205288.
- [18] M. Fabinger and J. McGreevy, “*On smooth time-dependent orbifolds and null singularities*,” hep-th/0206196.
- [19] S. Elitzur, A. Giveon, D. Kutasov, and E. Rabinovici, “*From big bang to big crunch and beyond*,” *JHEP* **06** (2002) 017, hep-th/0204189.
- [20] B. Craps, D. Kutasov, and G. Rajesh, “*String propagation in the presence of cosmological singularities*,” *JHEP* **06** (2002) 053, hep-th/0205101.
- [21] J. Simon, “*Null orbifolds in AdS, time dependence and holography*,” *JHEP* **10** (2002) 036, hep-th/0208165.
- [22] O. Aharony, M. Fabinger, G. T. Horowitz, and E. Silverstein, “*Clean time-dependent string backgrounds from bubble baths*,” *JHEP* **07** (2002) 007, hep-th/0204158.
- [23] A. Buchel, P. Langfelder, and J. Walcher, “*On time-dependent backgrounds in supergravity and string theory*,” *Phys. Rev.* **D67** (2003) 024011, hep-th/0207214.
- [24] M. Alishahiha and S. Parvizi, “*Branes in time-dependent backgrounds and AdS/CFT correspondence*,” *JHEP* **10** (2002) 047, hep-th/0208187.
- [25] E. Dudas, J. Mourad, and C. Timirgaziu, “*Time and space dependent backgrounds from nonsupersymmetric strings*,” hep-th/0209176.

- [26] M. Berkooz, B. Craps, D. Kutasov, and G. Rajesh, “*Comments on cosmological singularities in string theory*,” hep-th/0212215.
- [27] A. J. Tolley and N. Turok, “*Quantum fields in a big crunch / big bang spacetime*,” *Phys. Rev.* **D66** (2002) 106005, hep-th/0204091.
- [28] C. Gordon and N. Turok, “*Cosmological perturbations through a general relativistic bounce*,” hep-th/0206138.
- [29] J. Figueroa-O’Farrill and J. Simon, “*Supersymmetric Kaluza-Klein reductions of M2 and M5 branes*,” hep-th/0208107.
- [30] M. Fabinger and S. Hellerman, “*Stringy resolutions of null singularities*,” hep-th/0212223.
- [31] A. Hashimoto and S. Sethi, “*Holography and string dynamics in time-dependent backgrounds*,” *Phys. Rev. Lett.* **89** (2002) 261601, hep-th/0208126.
- [32] L. Cornalba and M. S. Costa, “*On the classical stability of orientifold cosmologies*,” hep-th/0302137.
- [33] S. W. Hawking, “*The Chronology protection conjecture*,” *Phys. Rev.* **D46** (1992) 603–611.
- [34] M. Visser, “*The quantum physics of chronology protection*,” gr-qc/0204022.
- [35] B. S. Kay, “*The principle of locality and quantum field theory on (nonglobally hyperbolic) curved space-times*,” *Rev. Math. Phys.* **SI1** (1992) 167.
- [36] A. Chamblin and G. W. Gibbons, “*A judgement on spinors*,” *Class. Quant. Grav.* **12** (1995) 2243–2248, gr-qc/9504048.
- [37] A. Chamblin and G. W. Gibbons, “*Topology and time reversal*,” gr-qc/9510006.
- [38] E. K. Boyda, S. Ganguli, P. Horava, and U. Varadarajan, “*Holographic protection of chronology in universes of the Goedel type*,” hep-th/0212087.
- [39] C. A. R. Herdeiro, “*Spinning deformations of the D1-D5 system and a geometric resolution of closed timelike curves*,” hep-th/0212002.
- [40] T. Harmark and T. Takayanagi, “*Supersymmetric Gödel universes in string theory*,” hep-th/0301206.

- [41] E. G. Gimon and A. Hashimoto, “*Black holes in Gödel universes and pp-waves*,” hep-th/0304181.
- [42] L. Dyson, “*Chronology protection in string theory*,” hep-th/0302052.
- [43] E. Schrodinger, *Expanding Universes*. Cambridge, UK: Univ. Pr. (1956).
- [44] G. W. Gibbons, “*The elliptic interpretation of black holes and quantum mechanics*,” *Nucl. Phys.* **B271** (1986) 497.
- [45] N. Sanchez, “*Quantum field theory and the ‘Elliptic Interpretation’ of de Sitter spacetime*,” *Nucl. Phys.* **B294** (1987) 1111.
- [46] M. K. Parikh, I. Savonije, and E. Verlinde, “*Elliptic de Sitter space: $dS/Z(2)$* ,” *Phys. Rev.* **D67** (2003) 064005, hep-th/0209120.
- [47] N. D. Birrell and P. C. W. Davies, *Quantum Fields in Curved Space*. Cambridge Univ. Press (1982).
- [48] J. Polchinski, *String theory. Vol. 1: An introduction to the bosonic string*. Cambridge Univ. Press (1998).
- [49] F. Larsen, A. Naqvi, and S. Terashima, “*Rolling tachyons and decaying branes*,” *JHEP* **02** (2003) 039, hep-th/0212248.
- [50] S. D. Mathur, “*Is the Polyakov path integral prescription too restrictive?*,” hep-th/9306090.
- [51] M. B. Green, J. H. Schwarz, and E. Witten, *Superstring Theory. Vol. 1: Introduction*. Cambridge Univ. Press (1987).
- [52] A. J. Niemi and G. W. Semenoff, “*Finite temperature quantum field theory in Minkowski space*,” *Ann. Phys.* **152** (1984) 105.
- [53] P. Kraus, H. Ooguri and S. Shenker, “*Inside the horizon with AdS/CFT*,” hep-th/0212277.
- [54] J. S. Schwinger, “*Brownian motion of a quantum oscillator*,” *J. Math. Phys.* **2** (1961) 407–432.
- [55] L. V. Keldysh, “*Diagram technique for nonequilibrium processes*,” *Zh. Eksp. Teor. Fiz.* **47** (1964) 1515–1527.